Analysis and Control of Primary Resonance in an Oscillatory Cantilever Beam Excited Transversely at Its Free End

Ali Kandil, Eman Desoky and Magdy Kamel

***Abstract*—In this paper, an oscillatory cantilever beam that is excited transversely at its free end is studied. This type of excitation causes the appearance of external and parametric forces that enhance the unwanted nonlinear vibrations of the beam especially at resonance cases. This dynamical behavior is modeled in a nonlinear differential equation to be solved analytically and numerically in an approximate sense. In addition, positive position feedback (PPF) control algorithm is applied through piezoelectric actuators implemented all over the beam's surface in order to reduce such vibrations. Furthermore, the simultaneous primary and internal $1:1$ resonance case is investigated to see how the control law can overcome it. The beam's overall characteristics are pictured with the aid of the multiple scales method in order to judge the effectiveness of the controller. Accordingly, the steady-state behavior's stability is tested applying Lyapunov's first (indirect) method along with Routh-Hurwitz criterion. The bifurcation analysis of the cantilever beam is shown before and after control with comparing the beam's behavior pre and post control. Numerical verifications have been conducted in order to certify the applied control algorithm via time responses and phase portraits.**

***Keywords—Cantilever beam; saddle-node bifurcation; simultaneous resonance; positive position feedback; phase plane*.**

Nomenclature

$y, \dot{y}, \ddot{y}$	Cantilever beam's displacement, velocity, and acceleration
$z, \dot{z}, \ddot{z}$	PPF's displacement, velocity, and acceleration
c, μ	Linear viscous damping parameters of the beam and PPF
$\sqrt{\beta_y}$, $\sqrt{\beta_c}$	Angular frequencies of the beam and PPF
α_2, α_3	Cubic-nonlinearity parameters of the beam
α_1	Parametric excitation parameter of the beam
$F_1, \bar{F}_1$	Parametric excitation force amplitudes
Ω_1	Parametric excitation force frequency
f	Amplitude of the exciting external force
Ω_2	Angular frequency of the exciting external force
k, γ	Gains of the z and y signals

I. INTRODUCTION

Nonlinear dynamics occurring in the cantilever beams is an important topic due to its importance in several applications of civil engineering, mechanical engineering, spacecraft stations, and satellite antennas. Some of the cantilever beam's mathematical models are nonlinear differential equations with periodic-type coefficients, and these differential equations are often found in parametrically excited beams. Oueini and Nayfeh [1] provided a cubic velocity feedback control for a parametrically-excited cantilever beam where the response's amplitude was mitigated by the proposed control algorithm through mathematical and experimental analysis. Pantographs [2] and asymmetric rotors [3] are typical examples of engineering systems that confronted a parametric resonance excitation force. However, that type of excitation was utilized in energy harvesting [4]. Additional systems were analyzed and exploited for suppressing the vibrations and studying the stability as in the parametrically-excited viscoelastic beam by Zhang et al. [5]. They explored the time-varying axial tension which was the reason for parametric excitation happened nearly at twice the natural frequency of the studied model. In order to suppress the horizontal oscillations of a suspended body represented by a nonlinear ODE, El-Ganaini et al. [6] In order to finish the task with analyzing the impacts of time delay on the entire control operation, a time-delayed positive position feedback controller was built. designing the PPF's natural frequency to match the motion's natural frequency of the levitated body. Ferrari and Amabili [7] used four pairs of approximately collinear piezoelectric sensors and actuators to control four normal modes. Some limitations were evident in the experimental findings of the control, particularly in the MIMO implementation with the applied PPF algorithm.

Recently, researchers have been scoping on the discipline of chaos. Zhang [8] investigated the non-planar chaotic vibrations of a cantilever beam subjected to a mixture of axial and transverse excitations using normal form theory, Galerkin's technique, and perturbation methods. Regarding

Manuscript received [8 December 2024]; revised [13 February 2025]; accepted [7 March 2025]. Date of publication [1 July 2025]. (*Corresponding* author: Eman Desoky).

Ali Kandil,, Department of Applied and Computational Mathematics, Institute of Basic and Applied Sciences, Egypt-Japan University of Science and Technology (E-JUST), New Borg El-Arab City, 21934, Alexandria, Egypt; and Department of Physics and Engineering Mathematics, Faculty of Electronic Engineering, Menouf, 32952, Menoufia University, Egypt; (ali.kandil@ejust.edu.eg)

Eman Desoky, Department of Basic Science, Menoufia Higher Institute of Engineering and Technology, El-Bagour, 32821, Egypt; (emandesoky51@gmail.com)

Magdy Kamel, Department of Physics and Engineering Mathematics, Faculty of Electronic Engineering, Menouf, 32952, Menoufia University, Egypt; (dr_magdi_kamel@yahoo.com).

high-injection strength, Mengue and Essimbi [9] represented the bifurcations of an optically-injected semiconductor lasers by the bifurcation diagrams where different types of bifurcation points appeared and the bursting behavior as well. The predator-prey of discrete-time model was presented in a Holing type IV functional response by Rana and Kulsum [10] where the model exhibited chaotic behavior and multi-periodic orbits. Kandil et al. [11-13] investigated the time delay effects on the PPF vibration control of a rotating blade's oscillations. They modified the form of PPF in order to eliminate the drawbacks of the classical one and to enhance the operation of the adaptive one where the idea case (zero-time-delay) and the practical case (non-zero-time-delay) were studied. Yang and Jiang [14] worked on the duffing oscillator under the effects of external excitation and a degenerate saddle point in order to formulate a chaos criterion using the method of Melnikov. Additional nonlinear dynamical models of flexible cantilever beams adopted using PPF control strategy variously for suppressing the high-amplitude vibrations done in [15-19]. Li et al. [20] focused their study on a cantilever micro-beam made of nickel where its nonlinear vibrations was measured by a non-contact system in order to test for the value of the fundamental natural frequency near the primary resonance case. Kumar [21] analyzed by experiment the effect of transvers harmonic excitations on the dynamical behavior of a cantilever beam. In addition, a finite element analysis was conducted considering the curvature and inertial nonlinearities for verifying the experimental work. Kandil et al. [22-23] proposed an adaptation mechanism for tuning the PPF controller applied on different engineering models in order to eliminate the classical peaks that were present in the behavior of the classical PPF. They enhanced their discussion with 2D and 3D visualizations for viewing the controllability regions in a wider aspect to the reader. Yakovleva et al. [24] derived a model of a Nano-structural beam whose shear stiffness was low subjected to a distributed transversal load. They adopted the methods of Runge-Kutta, Newmark, Sano-Sawada, Kantz, Wolf, and Rosenstein in order to extract the Lyapunov exponents for testing the model's dynamical periodicity. Zhang et al. [25] improved a model of a two-segment deployable beam where the 2D translational deformations were involved rather than the traditional model where only 1D transversal deformations were involved. Omidi and Mahmoodi [26] suppressed the unwanted vibrations in smart structures using a nonlinear integral resonant controller where it was a flexible practical option. El-Sayed and Bauomy [27] applied dual PPF controllers for controlling vertical conveyors' undesired vibrations where they adopted the multiple scales method to derive the frequency response equations then they did a verification of the gained solutions by a numerical simulation. In addition, Niu et al. [28] proposed a fractional PPF for creating a wide variety of the controller's adjusted parameters. They did experimental investigations using the proposed control algorithm on a vertical tail connected to MFC piezoelectric actuator. Abualnaja et al. [29] studied and controlled the nonlinear vibrations of Van der Pol-Duffing-type oscillator under the effect of parametric and external exciting forces via nonlinear integral PPF controller. They adopted both analytical and numerical techniques in order to describe the behavior of the whole mechanism before and after applying the control algorithm. Furthermore, PPF controller was applied by Amer et al. [30] in order to mitigate the noisy vibrations of a suspended cable whose source is external and parametric exciting forces. They applied the multiple scales method and Rung-Kutta technique to examine the worst resonance case occurring in the studied model through variating all different parameters. Farokhi et al. [31] studied the vibrations of a tip-mass cantilever beam subjected to parametric resonant force where a high-speed camera was used to catch the deformed deflections of the beam in only one period of equilibrium oscillations. Eman at el. [32] studied The oscillations of a cantilever beam with transversely energized free under external and parametric excitation forces. To reduce these vibrations, the Nonlinear Saturation Controller (NSC) algorithm is applied using a piezoelectric (PZT) actuator.

In this study, a nonlinear cantilever beam model is presented under the effect of external and parametric exciting forces where the generated vibrations are reduced using PPF controller. The approximate analytical solution and the frequency-response equations are derived utilizing the multiple scales method [33-34]. The equilibrium solutions' stability, near the simultaneous internal and primary resonance case, is tested and investigated. Numerical integration, using Rung-Kutta technique, is fulfilled to gain the approximate numerical solution besides examining the effects of varying all parameters on the frequency-response curves of the vibrating beam. Eventually, some conclusions are included to give recommendations about the applied control technique showing its advantages and drawbacks. The new contribution in this work is to suppress the high-amplitude vibration at the beam's free end using PPF controller. A high reduction ratio is reached at some specific conditions of the whole system.

II. MATHEMATICAL ANALYSIS ON THE CANTILEVER BEAM'S MOTION

The nonlinear dynamical model of the studied cantilever beam is presented in this section. A PPF controller algorithm is shown in Figure (1) where it can be coupled to the beam's model with the help of piezoelectric configuration. The cantilever beam's equation of motion as stated in Ref. [8] is written as follows:

$$\ddot{y} + c\dot{y} + \beta_y y - 2\alpha_1 F_1 \cos(\Omega_1 t)\, y + \alpha_2 y(y\ddot{y} + \dot{y}^2) + \alpha_3 \beta_y y^3 - 2\bar{F}_1 \cos(\Omega_1 t)\, y^3 = f\cos(\Omega_2 t) \quad (1)$$

Applying the nonlinear PPF controller to Equation (1), the modified beam's equation will be

$$\ddot{y} + c\dot{y} + \beta_y y - 2\alpha_1 F_1 \cos(\Omega_1 t)\, y + \alpha_2 y(y\ddot{y} + \dot{y}^2) + \alpha_3 \beta_y y^3 - 2\bar{F}_1 \cos(\Omega_1 t)\, y^3 = f\cos(\Omega_2 t) + kz \quad (2)$$

$$\ddot{z} + \mu\dot{z} + \beta_c z = \gamma y \quad (3)$$

To obtain a scaled system of equations which is suitable for applying the method of multiple scales, scale transformations can be used as

$$\alpha_1 = \varepsilon\alpha_1,\ \alpha_2 = \varepsilon\alpha_2,\ \alpha_3 = \varepsilon\alpha_3,\ \bar{F}_1 = \varepsilon\bar{F}_1,\ c = \varepsilon c,\ f = \varepsilon f,\ k = \varepsilon k,\ \gamma = \varepsilon\gamma,\ \mu = \varepsilon\mu \quad (4)$$

where ε $(0 < \varepsilon \ll 1)$ is a small perturbation parameter. In addition, β_y and β_c can be replaced by ω^2 and ω_c^2 in the next stage of analysis.

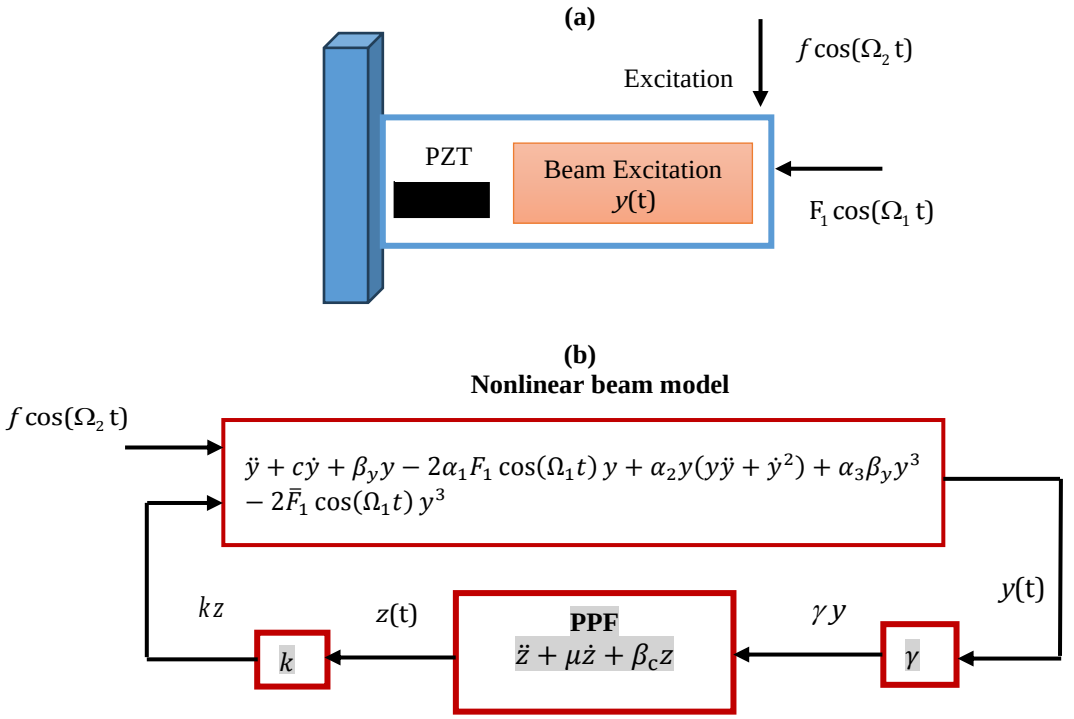

Figure 1. (a) Cantilever beam with piezoelectric configuration, (b) the controlled cantilever beam block diagram.

By substituting Equation (4) into Equations. (2) and (3), Under coupled parametric and driving excitation, we arrive at the following dimensionless two-degrees of freedom nonlinear system:

$$\ddot{y} + \varepsilon c\dot{y} + \omega^2 y - 2\varepsilon\alpha_1 F_1\cos(\Omega_1 t)\, y + \varepsilon\alpha_2 y(y\ddot{y} + \dot{y}^2) + \varepsilon\alpha_3\omega^2 y^3 - 2\varepsilon\bar{F}_1\cos(\Omega_1 t)\, y^3 = \varepsilon f\cos(\Omega_2 t) + \varepsilon kz \quad (5)$$

$$\ddot{z} + \varepsilon\mu\dot{z} + \omega_c^2 z = \varepsilon\gamma y \quad (6)$$

We seek a first-order uniform solution of Equations. (5) and (6), by using multiple scales method [32, 33] as:

$$y(t,\varepsilon) = y_0(T_0, T_1) + \varepsilon y_1(T_0, T_1) + \cdots \quad (7.a)$$

$$z(t,\varepsilon) = z_0(T_0, T_1) + \varepsilon z_1(T_0, T_1) + \cdots \quad (7.b)$$

where $T_0 = t$ and $T_1 = \varepsilon t$ are the adopted time scales. The time derivatives in terms of T_0 and T_1, will take the form

$$\frac{d}{dt} = \frac{\partial}{\partial T_0}\frac{\partial T_0}{\partial t} + \frac{\partial}{\partial T_1}\frac{\partial T_1}{\partial t} = D_0 + \varepsilon D_1 \quad (8.a)$$

$$\frac{d^2}{dt^2} = D_0^2 + 2\varepsilon D_0 D_1 + \varepsilon^2 D_1^2 \quad (8.b)$$

Substituting Equations. (7) and (8) into (5) and (6) and equating the coefficients of ε on both sides give the following

$O(\varepsilon^0)$:

$$D_0^2 y_0 + \omega^2 y_0 = 0 \quad (9.a)$$

$$D_0^2 z_0 + \omega_c^2 z_0 = 0 \quad (9.b)$$

and, $O(\varepsilon^1)$:

$$\begin{aligned} D_0^2 y_1 + \omega^2 y_1 = {} & -2D_0 D_1 y_0 - cD_0 y_0 - \alpha_2 y_0^2 D_0^2 y_0 \\ & + 2\alpha_1 F_1\cos(\Omega_1 t)\, y_0 - \alpha_2 y_0 (D_0 y_0)^2 \\ & - \alpha_3\omega^2 y_0^3 + 2\bar{F}_1\cos(\Omega_1 t)\, y_0^3 \\ & + f\cos(\Omega_2 t) + kz_0 \end{aligned} \quad (10.a)$$

$$D_0^2 z_1 + \omega_c^2 z_1 = -2D_0 D_1 z_0 - \mu D_0 z_0 + \gamma y_0 \quad (10.b)$$

Equations (9) have a solution in the form

$$y_0 = Ae^{i\omega T_0} + \bar{A}e^{-i\omega T_0} \quad (11.a)$$

$$z_0 = A_1 e^{i\omega_c T_0} + \bar{A}_1 e^{-i\omega_c T_0} \quad (11.b)$$

where the over-barred terms denote the complex conjugate of the same term. Substituting Equations. (11) into Equations. (10), the following solutions are obtained

$$\begin{aligned} D_0^2 y_1 + \omega^2 y_1 = {} & -2[i\omega A' e^{i\omega T_0}] - c[i\omega A e^{i\omega T_0}] \\ & + \alpha_1 F_1 A\left[e^{i(\omega+\Omega_1)T_0} + e^{i(\omega-\Omega_1)T_0}\right] \\ & + \bar{F}_1 A^3 e^{i(3\omega+\Omega_1)T_0} \\ & - \alpha_2\omega^2[A^3 e^{3i\omega T_0} + 3\bar{A}A^2 e^{i\omega T_0}] \\ & + \alpha_2\omega^2[A^3 e^{3i\omega T_0} - A^2\bar{A}e^{i\omega T_0}] \\ & + 3\bar{F}_1 A^2\bar{A}e^{i(\omega+\Omega_1)T_0} - 3\alpha_3\omega^2 A^2\bar{A}e^{i\omega T_0} \\ & - \alpha_3\omega^2 A^3 e^{3i\omega T_0} + \frac{f}{2}e^{i\Omega_2 T_0} \\ & + k[A_1 e^{i\omega_c T_0}] + c.c. \end{aligned} \quad (12.a)$$

$$\begin{aligned} D_0^2 z_1 + \omega_c^2 z_1 = {} & -2D_1[i\omega_c A_1 e^{i\omega_c T_0}] - \mu i\omega_c A_1 e^{i\omega_c T_0} \\ & + \gamma A e^{i\omega T_0} + c.c. \end{aligned} \quad (12.b)$$

where $c.c.$ denotes the complex conjugates of the preceding terms. The worst resonance case that was deduced form Equations. (12), is the simultaneous resonance ($\Omega_2 = \omega = \omega_c$). By using the detuning parameters σ_1 and σ_2, the proximity of the simultaneous resonance can be quantitatively defined as

$$\Omega_2 = \omega + \varepsilon\sigma_1 \quad (13.a)$$

$$\omega_c = \omega + \varepsilon\sigma_2 \quad (13.b)$$

Substituting Equations. (13) into Equations. (12), then eliminating the secular terms for y and z solutions in order to get the following solvability conditions

$$-2i\omega A' - ci\omega A + 2\alpha_2\omega^2 A^2\bar{A} - 3\alpha_3\omega^2 A^2\bar{A} + \frac{f}{2}e^{i\sigma_1 T_1} + kA_1 e^{i\sigma_2 T_1} = 0 \quad (14.a)$$

$$-2i\omega_c A_1' e^{i\sigma_2 T_1} - \mu i\omega_c A_1 e^{i\sigma_2 T_1} + \gamma A = 0 \quad (14.b)$$

It is convenient to express $A(T_1)$ and $A_1(T_1)$ in the complex polar form.

$$A = \frac{a_1}{2} e^{ib_1} \tag{15.a}$$

$$A_1 = \frac{a_2}{2} e^{ib_2} \tag{15.b}$$

where a_1, a_2, b_1 and b_2 are real functions of T_1. By inserting Equations. (15) into (14), the following can be gained

$$-i\omega a_1' + \omega a_1 b_1' - \frac{1}{2} ci\omega a_1 + \frac{1}{4}\alpha_2 \omega^2 a_1^3 - \frac{3}{8}\alpha_3 \omega^2 a_1^3 + \frac{f}{2} e^{i(\sigma_1 T_1 - b_1)} + \frac{1}{2} k a_2 e^{i(\sigma_2 T_1 + b_2 - b_1)} = 0 \tag{16}$$

$$-i\omega_c a_2' + \omega_c a_2 b_2' - \frac{1}{2}\mu i \omega_c a_2 + \frac{1}{2}\gamma a_1 e^{i(-\sigma_2 T_1 + b_1 - b_2)} = 0 \tag{17}$$

Separating real and imaginary parts from Equations. (16) and (17), we have

$$a_1' = -\frac{1}{2} c a_1 + \frac{f}{2\omega}\sin\phi_1 + \frac{1}{2\omega} k a_2 \sin\phi_2 \tag{18.a}$$

$$a_1 b_1' = -\frac{1}{4}\alpha_2 \omega a_1^3 + \frac{3}{8}\alpha_3 \omega a_1^3 - \frac{f}{2\omega}\cos\phi_1 - \frac{1}{2\omega} k a_2 \cos\phi_2 \tag{18.b}$$

$$a_2' = -\frac{1}{2}\mu a_2 - \frac{1}{2\omega_c}\gamma a_1 \sin\phi_2 \tag{18.c}$$

$$a_2 b_2' = -\frac{1}{2\omega_c}\gamma a_1 \cos\phi_2 \tag{18.d}$$

where

$$\sigma_1 T_1 - b_1 = \phi_1 \tag{19.a}$$

$$\sigma_2 T_1 + b_2 - b_1 = \phi_2 \tag{19.b}$$

Substituting the T_1-derivatives of Equations. (19) into (18) gives a modified autonomous system of differential equations

$$a_1' = -\frac{1}{2} c a_1 + \frac{f}{2\omega}\sin\phi_1 + \frac{1}{2\omega} k a_2 \sin\phi_2 \tag{20.a}$$

$$\phi_1' = \sigma_1 + \frac{1}{4}\alpha_2 \omega a_1^2 - \frac{3}{8}\alpha_3 \omega a_1^2 + \frac{f}{2\omega a_1}\cos\phi_1 + \frac{1}{2\omega a_1} k a_2 \cos\phi_2 \tag{20.b}$$

$$a_2' = -\frac{1}{2}\mu a_2 - \frac{1}{2\omega_c}\gamma a_1 \sin\phi_2 \tag{20.c}$$

$$\phi_2' = \sigma_2 + \frac{1}{4}\alpha_2 \omega a_1^2 - \frac{3}{8}\alpha_3 \omega a_1^2 + \frac{f}{2\omega a_1}\cos\phi_1 + \frac{1}{2\omega a_1} k a_2 \cos\phi_2 - \frac{1}{2\omega_c a_2}\gamma a_1 \cos\phi_2 \tag{20.d}$$

The above equations govern the fluctuations in the beam's motion amplitude and phase that characterize its output response.

III. Stability Test via Jacobian Matrix and Routh-Hurwitz Criterion

For obtaining the fixed points of Equations. (20), we put $a_1' = 0$ and $a_2' = \phi_1' = \phi_2' = 0$ to give us the beam's and the controller's steady-state amplitudes and phases as

$$\frac{f}{2\omega}\sin\phi_1 = \frac{1}{2} c a_1 + \frac{\omega_c}{2\omega\gamma a_1} k\mu a_2^2 \tag{21.a}$$

$$\frac{f}{2\omega}\cos\phi_1 = -\sigma_1 a_1 - \frac{1}{4}\alpha_2 \omega a_1^3 + \frac{3}{8}\alpha_3 \omega a_1^3 + \frac{\omega_c}{\gamma a_1 \omega}\sigma_1 k a_2^2 - \frac{\omega_c}{\gamma a_1 \omega}\sigma_2 k a_2^2 \tag{21.b}$$

$$\frac{1}{2\omega_c}\gamma a_1 \sin\phi_2 = -\frac{1}{2}\mu a_2 \tag{21.c}$$

$$\frac{1}{2\omega_c}\gamma a_1 \cos\phi_2 = -\sigma_1 a_2 + \sigma_2 a_2 \tag{21.d}$$

The beam's and controller's frequency response equations can be derived from Equations. (21) which takes the following form

$$\left(\frac{f}{2\omega}\right)^2 = \left(\frac{1}{2} c a_1 + \frac{\omega_c}{2\omega\gamma a_1} k\mu a_2^2\right)^2 + \left(-\sigma_1 a_1 - \frac{1}{4}\alpha_2 \omega a_1^3 + \frac{3}{8}\alpha_3 \omega a_1^3 + \frac{\omega_c}{\gamma a_1 \omega}\sigma_1 k a_2^2 - \frac{\omega_c}{\gamma a_1 \omega}\sigma_2 k a_2^2\right)^2 \tag{22}$$

$$\left(\frac{1}{2\omega_c}\gamma a_1\right)^2 = \left(\frac{1}{2}\mu a_2\right)^2 + (-\sigma_1 a_2 + \sigma_2 a_2)^2 \tag{23}$$

A Jacobian matrix is derived from Equations. (20) to assess the stability of the steady-state solutions using the resultant matrix's eigenvalues. This can be done by letting that

$$a_n = a_{n0} + a_{n1} \tag{24.a}$$

$$\phi_n = \phi_{n0} + \phi_{n1} \tag{24.b}$$

where a_{n0} and ϕ_{n0} satisfy Equations. (21), while a_{n1} and ϕ_{n1} are small-valued quantities compared to a_{n0} and ϕ_{n0}. Substituting Equations. (24) into (20) with linearizing the terms containing a_{n1} and ϕ_{n1} lead to

$$\begin{bmatrix} \dot{a}_{11} \\ \dot{\phi}_{11} \\ \dot{a}_{21} \\ \dot{\phi}_{21} \end{bmatrix} = [J] \begin{bmatrix} a_{11} \\ \phi_{11} \\ a_{21} \\ \phi_{21} \end{bmatrix} = \begin{bmatrix} u_{11} & u_{12} & u_{13} & u_{14} \\ u_{21} & u_{22} & u_{23} & u_{24} \\ u_{31} & u_{32} & u_{33} & u_{34} \\ u_{41} & u_{42} & u_{43} & u_{44} \end{bmatrix} \begin{bmatrix} a_{11} \\ \phi_{11} \\ a_{21} \\ \phi_{21} \end{bmatrix} \tag{25}$$

where the entries of the Jacobian matrix J are given in the appendix. The Jacobian matrix's characteristic equation is

$$\upsilon^4 + \xi_1 \upsilon^3 + \xi_2 \upsilon^2 + \xi_3 \upsilon + \xi_4 = 0 \tag{26}$$

where υ denotes the eigenvalue and $\xi_1, \xi_2, \xi_3, \xi_4$ are given in the appendix. Accordingly, if all the real parts of υ are negative, then the steady-state solution is stable. Otherwise, it is unstable. In addition, the necessary and sufficient criteria, according to Ruth-Hurwitz criterion, for all the roots in Equation (26), to have negative real parts are

$$\xi_1 > 0, \xi_1\xi_2 - \xi_3 > 0, \xi_3(\xi_1\xi_2 - \xi_3) - \xi_1\xi_4 > 0, \xi_4 > 0 \tag{27}$$

IV. Graphical Analysis on the Cantilever Beam's Motion

In this section, from Ref. [8], the selected values for the beam and controller parameters are chosen as: $\omega = 0.5$, $\sigma_2 = 0$, $\alpha_1 = 1$, $k = 0.1$, $\alpha_2 = 13.2$, $\omega_c = 0.5$, $\gamma = 0.1$, $\alpha_3 = 5.01$, $c = 0.011$, $F = -0.001$, $\bar{F} = 0.1$, $\mu = 0.001$, $\Omega_1 = 0.5$, unless otherwise stated. The upcoming graphical curves explain the relationship between the amplitude of response a and the beam's and the PPF's detuning settings with various exciting forces f. These curves show the stable solutions as solid lines and the unstable solutions as dashed lines. Figure (2) displays the main system's and the controller's frequency-response curves for various excitation force values f. In Figure (2a), the excitation force amplitude f determines the main system's steady-state amplitude, which is a monotonically growing function. The jump phenomena

appears as a result of the dominance of the nonlinearity, and the curve is bent to the left as the force amplitude increases, denoting a softening effect. The equilibrium amplitudes of the beam and PPF, in Figures (2b) and (2c), are directly proportional to the exciting force amplitude f. Two peaks are obtained one at $\sigma_1 = 0.1$ and the other at $\sigma_1 = -0.1$, so they are creating a canyon in between whose length is about 0.2 as depicted in the figure. This means that the effective operating interval for the PPF is approximately between the two values $\sigma_1 = \pm 0.1$, and the beam's steady-state amplitude is at its lowest level at $\sigma_1 = 0$. Also, the jump phenomena appear obviously for the PPF and the beam as depicted by the curves.

Figure (3) shows the effect of varying the control factor k on the frequency-response curves of the beam and the PPF. In Figures (3a) and (3b), the bandwidth between the produced two peaks are increasing monotonically with the control factor k. However, the beam's and PPF's peak amplitudes are not affected by changing the values of k.

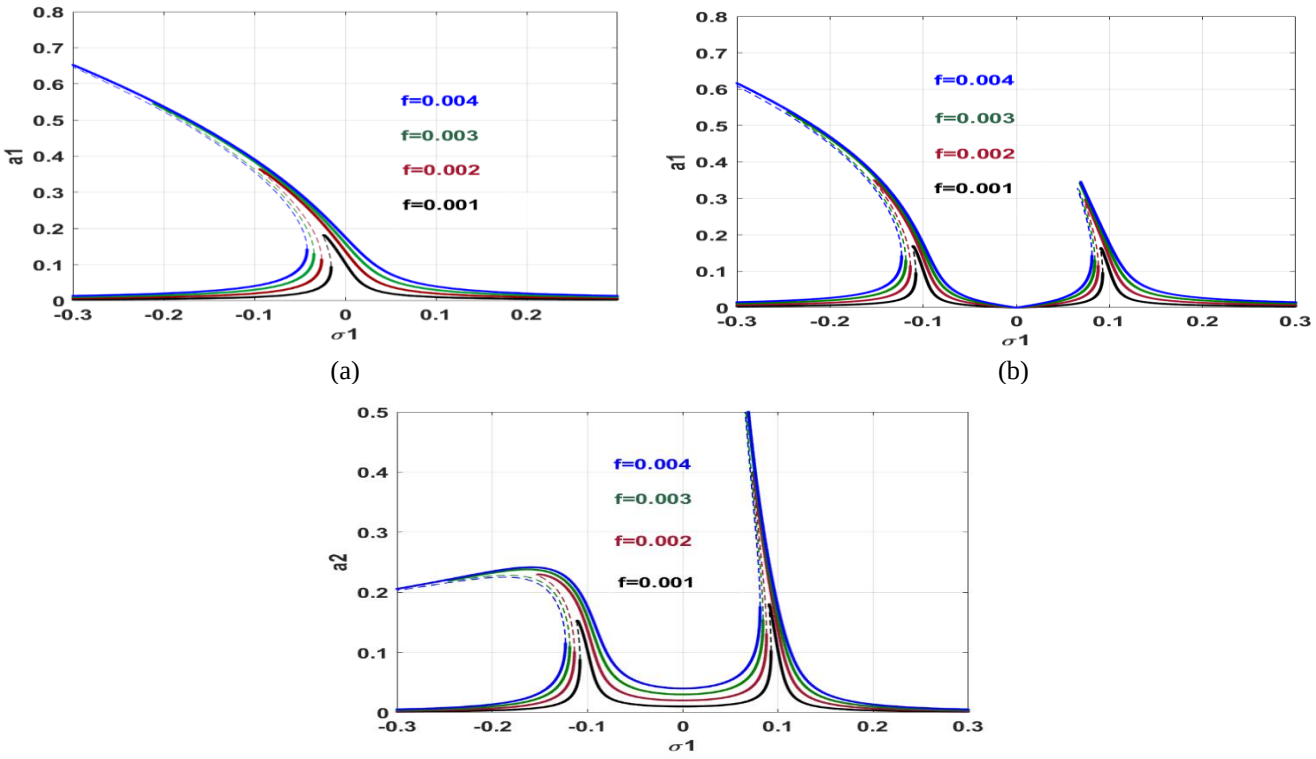

Figure 2. Frequency-response curves pre and post PPF control: (a) beam's amplitude pre-control, (b) beam's amplitude post-control, (c) PPF's amplitude.

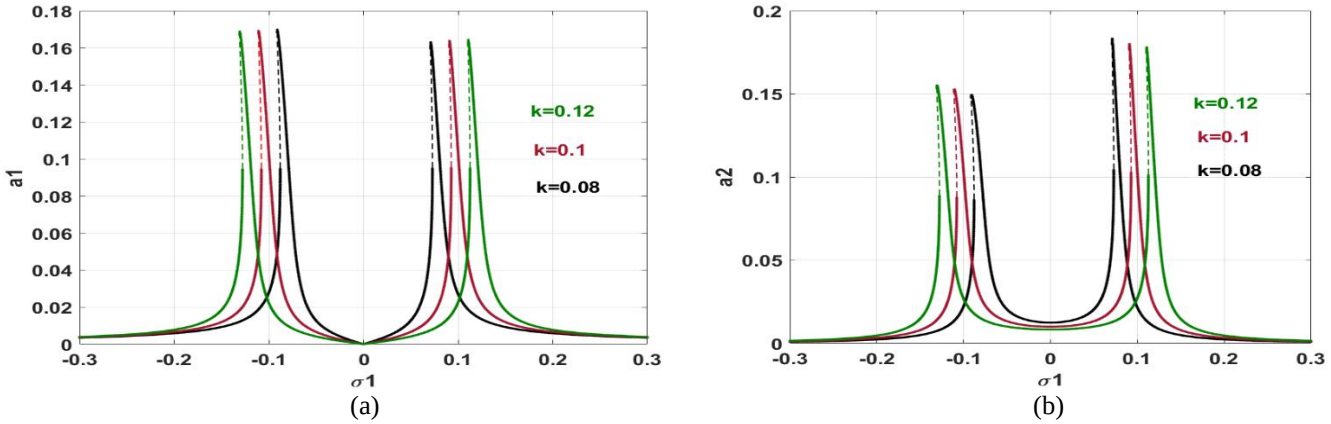

Figure 3. Frequency-response curves after PPF control at $f = 0.001$: (a) beam's amplitude pre-control, (b) PPF's amplitude.

The beam's and PPF's force-response curves are shown in Figures (4) and (5). Figure (4) clearly shows the relationship between the exciting force f and the beam's amplitude when $\sigma_1 = 0$, is nonlinear before control and the steady-state amplitude of the beam increases for a little push in the exciting force. After control, the relation becomes almost-horizontal and stable approaching the trivial case. The exciting force grows linearly as the PPF's amplitude rises. According to Figure (5), the beam's and PPF's amplitudes grow monotonically in both cases of pre and post control related to increasing the exciting force. The nonlinearity is dominant over the beam's response before and after control. Through the interval $-0.1 < \sigma_1 < 0$, of the detuning parameter before control, the beam's amplitude is unstable. After control, the amplitudes are unstable for an interval $0.07 < \sigma_1 < 0.1$, of the detuning parameter σ_1.

place table headings above the tables. Do not include captions as part of the figures, or put them in "text boxes" linked to the figures. Also, do not place borders around the outside of your figures.

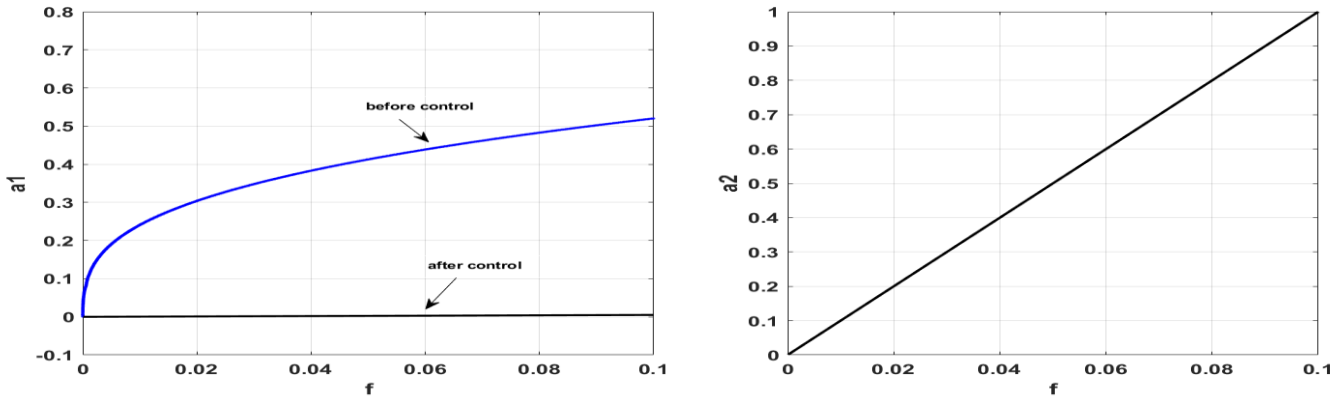

(a) (b)

Figure 4. Force-response curves pre and Post PPF control: (a) beam's amplitude pre- and post-control, (b) PPF's amplitude.

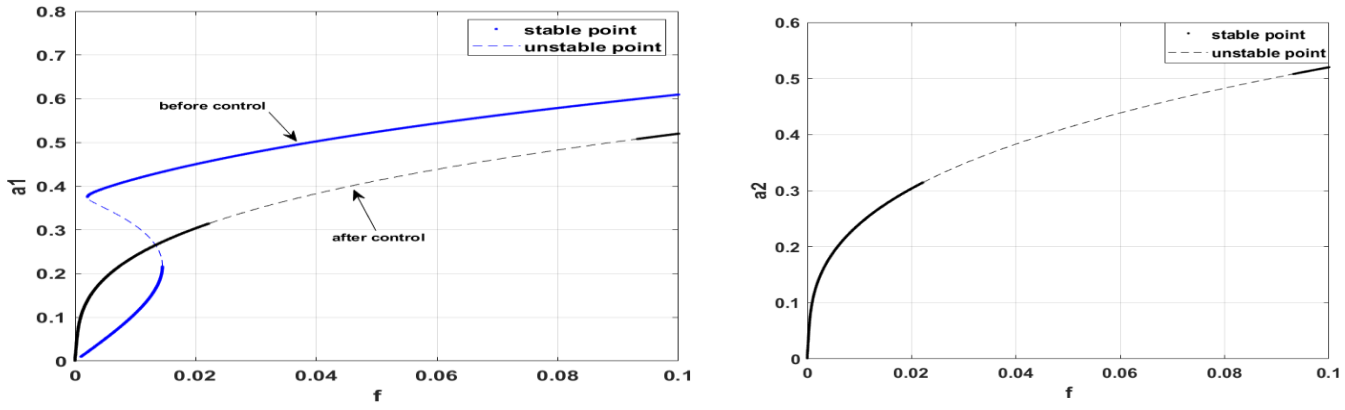

(a) (b)

Figure 5. Force-response curve at $\sigma_1 = -0.1$ pre and post PPF control: (a) beam's amplitude pre- and post-control, (b) PPF's amplitude.

Time history of the equilibrium amplitude of the uncontrolled and controlled beam near the simultanous resonance case $\Omega = \omega + \sigma_1$ and $\omega_c = \omega + \sigma_2$ (where $\Omega = \omega = \omega_c = 0.5$) are numerically simulated as shown in Figures (6) to (8) using the MATLAB command ODE45. At $f = 0.001$ ($\sigma_1 = \sigma_2 = 0$) according to Figure (6a), the beam's uncontrolled amplitude is approximately 0.105, while tends to zero for the controlled beam's amplitude in Figure (6b) and the PPF's amplitude is around 0.012. These results confirm a good agreement between the analytical and numerical solutions. In Figure (2a), the beam's uncontrolled amplitude is approximately 0.099, the controlled beam's amplitude is zero in Figure (2b) and the PPF's amplitude is around 0.0099 in Figure (2c). According to the phase portraits of Figures (6b), (6d), and (6f), the uncontrolled beam, the controlled beam, and the PPF all have stable steady-state amplitudes. The controller effectiveness for this resonance case is about 105. This means that the oscillations have neen reduced by about 99%.

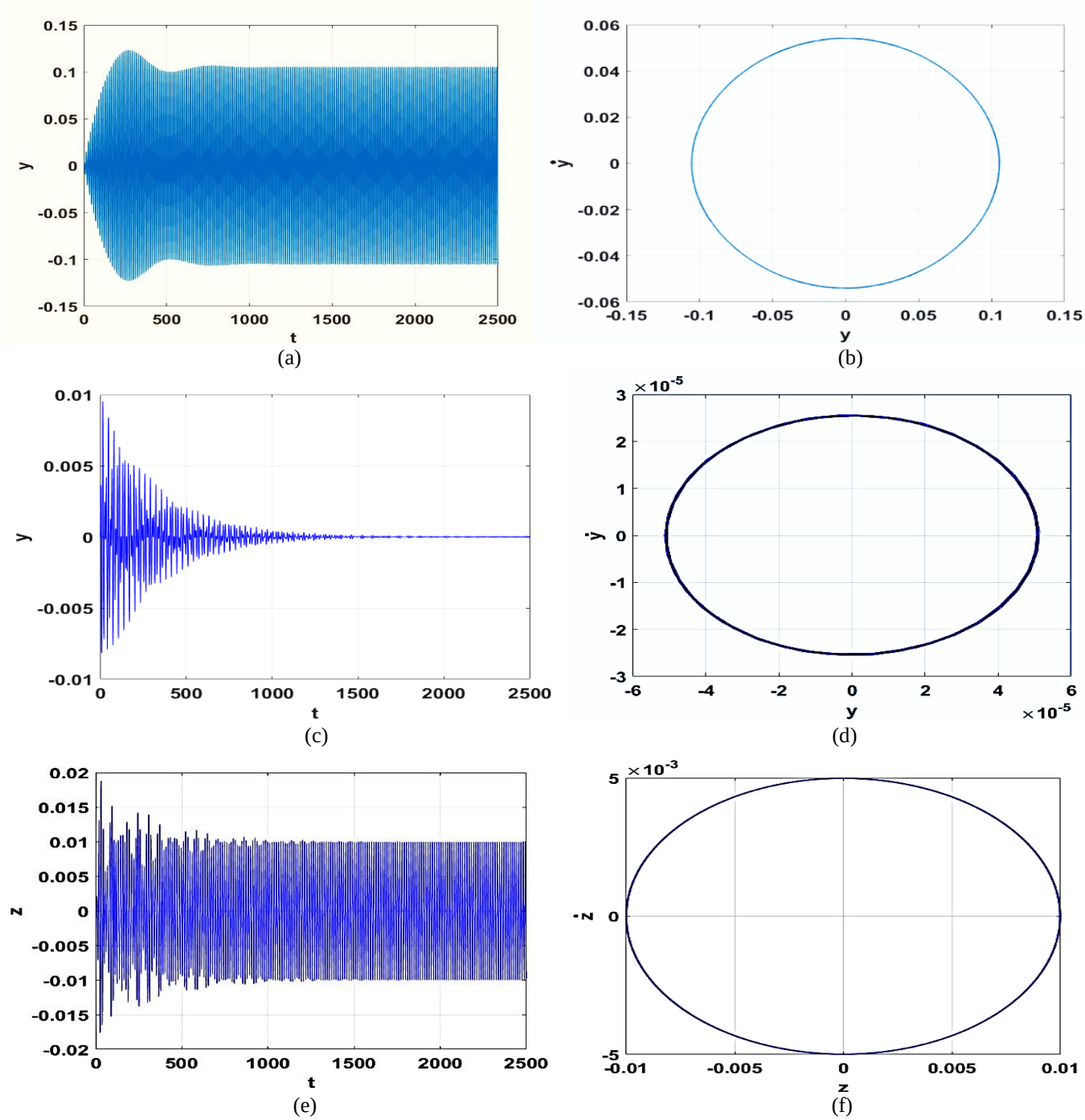

Figure 6. The cantilever beam's time-vibrations before and after control for $f = 0.001$: (a, b) the beam's time response and phase plane before control; (c, d) the beam's time response and phase plane after control; (e, f) time reponse and phase plane of the PPF.

At $f = 0.004$ ($\sigma_1 = \sigma_2 = 0$) according to Figure (7a), the uncontrolled beam has an amplitude of around 0.177, whereas the controlled beam, shown in Figure (7b), has an amplitude that tends to about zero and is approximately 0.055. According to the phase plane of Figures (7a), (7b), and (7c), the steady-state amplitude of the beam and the PPF are all stable. These results confirm a good agreement between the analytical and numerical solutions. In Figure (2a), the beam's uncontrolled amplitude is approximately 0.175, the controlled beam's amplitude is zero in Figure (2b) and the PPF's amplitude is around 0.0399 in Figure (2c).

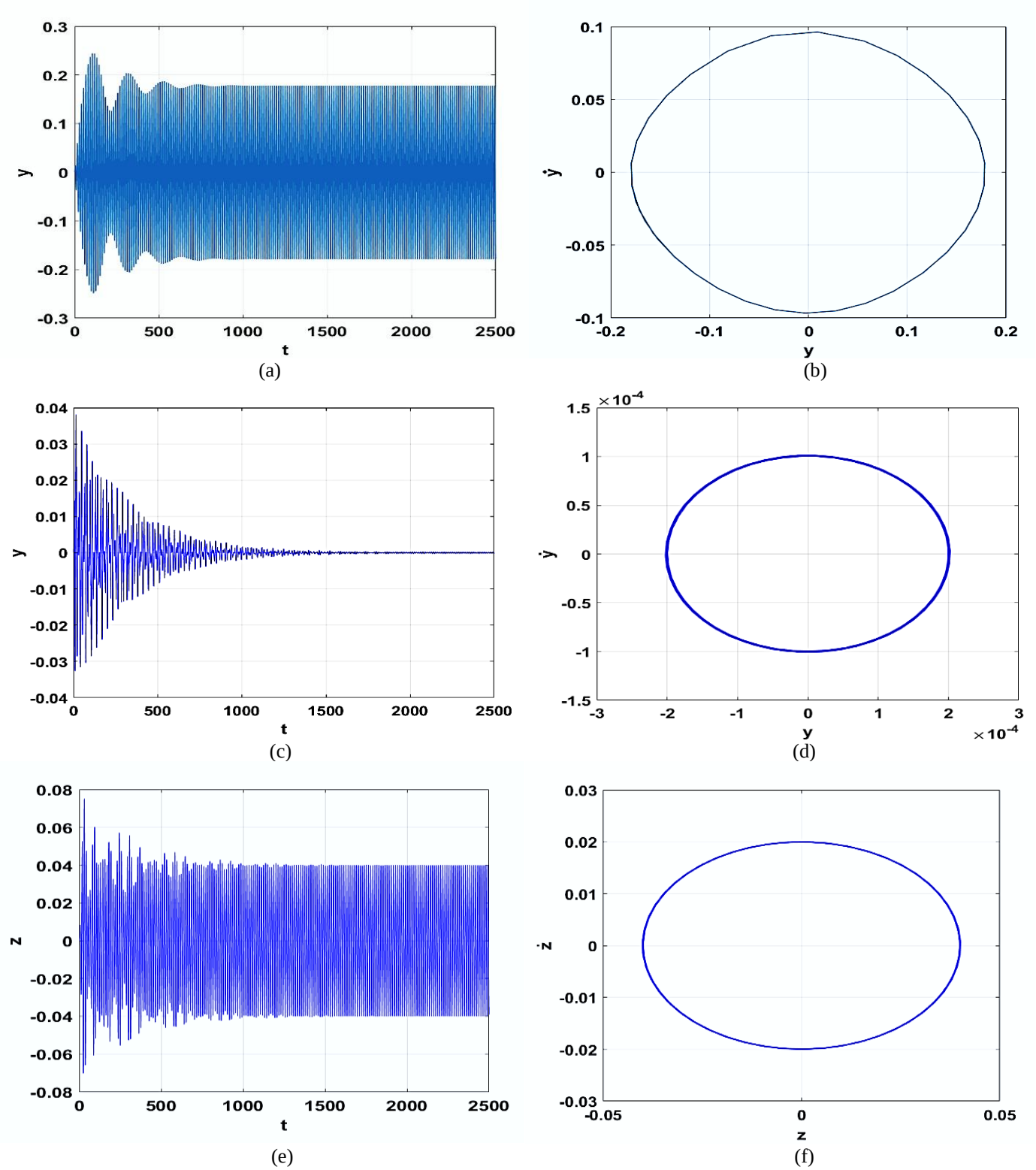

Figure 7. The cantilever beam's time-vibrations before and after control for $f = 0.004$:(a, b) the beam's time response and phase plane before control; (c, d) the beam's time response and phase plane after control; (e, f) time response and phase plane of the PPF.

At $f = 0.0222$ ($\sigma_1 = -0.1$, $\sigma_2 = 0$), the uncontrolled beam's amplitude is around 0.24, and it stabilizes as depicted in Figure (8a). But the amplitude of the controlled beam and the PPF become unstable as shown in the phase portraits of Figures (8b) and (8c). This means that the force f should not exceed 0.0222 in the controlled case.

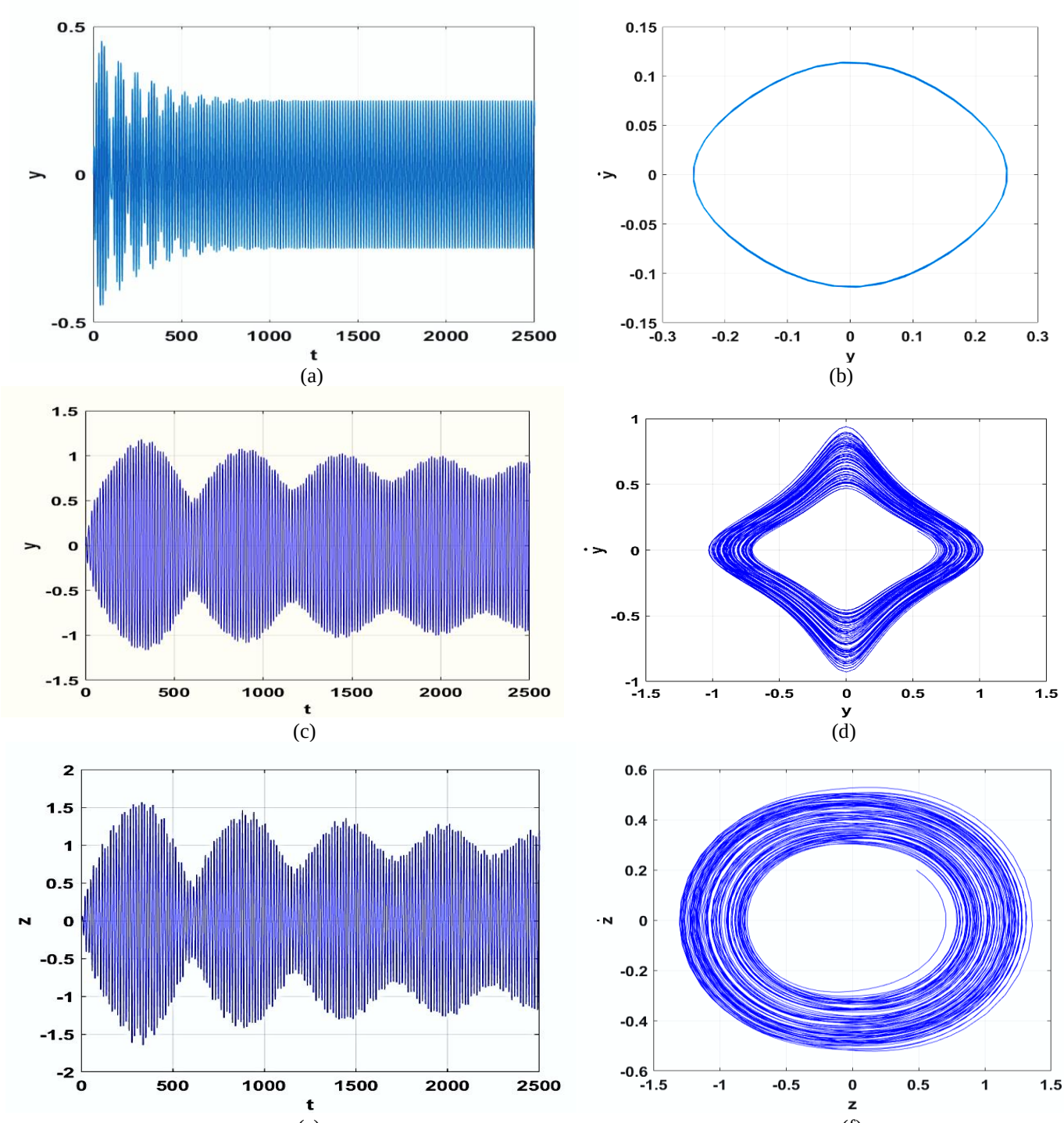

Figure 8. The cantilever beam's time-vibrations before and after control for $\sigma_1 = -0.1$, $f = 0.0222$: (a, b) the beam's time reponse and phase plane before control; (c, d) the beam's time response and phase plane after control; (e, f) time history and phase plane of the PPF.

V. CONCLUSION

This work discussed the analysis and control of the nonlinear oscillations in a parametrically-excited dynamical cantilever beam system at its free end. We applied PPF control in this model and extracted analysis of the equation before and after control. Several responses showing the dynamical behavior were included under control. Finally, we compared between the analytical and the numerically results before and after control. These results can be summarized in the following points:

1. Before control, the cantilever beam system suffered from high vibration amplitudes and jump phenomenon due to bifurcation points making the system unstable in some conditions.
2. After control, the system became more stable but there was some jumps and quite high vibration amplitudes.
3. The system vibrations reached minimum levels in range $\sigma_1 \in [-0.08, 0.08]$ especially at $\sigma_1 = 0$.
4. To increase bandwidth stability, we increased the gain of controller to make the system more stable.
5. The controlled system became stable when the force amplitude was small until reaching $f = 0.0222$.
6. When the force amplitude reached 0.0222, the model exhibited unstable behavior which was a drawback of the proposed controller at large force amplitudes.

Finally, we reached better reduction ratio than previous published research, as the reduction ratio for PPF controller reach 99%, while previously published research [32] reaches 89%, and this means that PPF controller is more suitable for the cantilever beam.

VI. SUGGESTIONS FOR FUTURE WORK

In the following, we introduce some suggestions for further developments:

1. Studying more complicated nonlinear dynamical systems that inherently have fractional order terms.
2. Involving experimental data to make more verification for the applied control strategies.
3. Searching for up-to-date control algorithms that enhance the control process more and more.
4. The proposed control strategies need to be tested on real-life structures like helicopter blades, robot manipulators and jet engine rotating blades.

VII. APPENDIX

The entries of the Jacobian matrix J in Eq. (25):

$$u_{11} = -\frac{1}{2}c$$
$$u_{12} = \frac{f}{2\omega}\cos\phi_{10}$$
$$u_{13} = \frac{1}{2\omega}k\sin\phi_{20}$$
$$u_{14} = \frac{1}{2\omega}ka_{20}\cos\phi_{20}$$
$$u_{21} = \frac{3}{4}\alpha_2\omega a_{10} - \frac{9}{8}\alpha_3\omega a_{10} + \frac{\sigma_1}{a_{10}}$$
$$u_{22} = -\frac{f}{2\omega a_{10}}\sin\phi_{10}$$
$$u_{23} = \frac{1}{2\omega a_{10}}k\cos\phi_{20}$$
$$u_{24} = -\frac{1}{2\omega a_{10}}ka_{20}\sin\phi_{20}$$
$$u_{31} = -\frac{1}{2\omega_c}\gamma\sin\phi_{20}$$
$$u_{32} = 0$$
$$u_{33} = -\frac{1}{2}\mu$$
$$u_{34} = -\frac{1}{2\omega_c}\gamma a_{10}\cos\phi_{20}$$
$$u_{41} = \frac{3}{4}\alpha_2\omega a_{10} - \frac{9}{8}\alpha_3\omega a_{10} + \frac{2\sigma_1}{a_{10}} - \frac{\sigma_2}{a_{10}}$$
$$u_{42} = -\frac{f}{2\omega a_{10}}\sin\phi_{10}$$
$$u_{43} = \frac{\omega_c k}{\omega\gamma a_{10}^2}(-\sigma_1 a_{20} + \sigma_2 a_{20}) + \frac{1}{a_{20}^2}(-\sigma_1 a_{20} + \sigma_2 a_{20})$$
$$u_{44} = \frac{k\omega_c}{2\gamma\omega a_{10}^2}\mu a_{20}^2 - \frac{1}{2}\mu$$

The coefficients of Eq. (26):

$$\xi_1 = -u_{11} - u_{22} - u_{33} - u_{44}$$
$$\xi_2 = -u_{12}u_{21} + u_{11}u_{22} + u_{33}u_{11} + u_{11}u_{44} + u_{33}u_{22} + u_{44}u_{22} - u_{34}u_{43} - u_{42}u_{24} - u_{23}u_{32} - u_{13}u_{31} - u_{14}u_{42} - u_{14}u_{41}$$
$$\xi_3 = -u_{11}u_{33}u_{22} - u_{11}u_{44}u_{22} + u_{11}u_{34}u_{43} - u_{33}u_{44}u_{22} - u_{11}u_{42}u_{24} - u_{22}u_{33}u_{44} + u_{34}u_{43}u_{22} + u_{11}u_{23}u_{32} + u_{23}u_{32}u_{44} - u_{23}u_{34}u_{42} - u_{24}u_{32}u_{43} + u_{24}u_{33}u_{42} + u_{12}u_{21}u_{33} + u_{12}u_{21}u_{44} - u_{12}u_{23}u_{31} - u_{12}u_{24}u_{41} - u_{13}u_{32}u_{21} + u_{13}u_{22}u_{31} + u_{13}u_{31}u_{44} - u_{13}u_{34}u_{41} - u_{14}u_{21}u_{42} + u_{14}u_{22}u_{42} - u_{14}u_{31}u_{43} + u_{14}u_{42}u_{33}$$
$$\xi_4 = u_{11}u_{22}u_{33}u_{44} - u_{11}u_{34}u_{43}u_{22} - u_{11}u_{23}u_{32}u_{44} - u_{11}u_{23}u_{34}u_{42} - u_{11}u_{24}u_{32}u_{43} - u_{11}u_{24}u_{33}u_{42} - u_{12}u_{21}u_{33}u_{44} + u_{12}u_{21}u_{34}u_{43} + u_{12}u_{23}u_{31}u_{44} - u_{12}u_{23}u_{34}u_{41} - u_{12}u_{24}u_{31}u_{43} + u_{12}u_{24}u_{41}u_{33} + u_{13}u_{21}u_{32}u_{44} - u_{13}u_{21}u_{34}u_{42} - u_{13}u_{22}u_{31}u_{44} + u_{13}u_{22}u_{34}u_{41} + u_{13}u_{24}u_{31}u_{42} - u_{13}u_{24}u_{32}u_{41} - u_{14}u_{21}u_{32}u_{43} + u_{14}u_{21}u_{42}u_{33} + u_{14}u_{22}u_{31}u_{43} - u_{14}u_{22}u_{42}u_{33} - u_{14}u_{23}u_{31}u_{42} + u_{14}u_{23}u_{32}u_{41}$$

REFERENCES

[1] Oueini, S.S., Nayfeh, A.H.: Single-mode control of a cantilever beam under principal parametric excitation. J. Sound Vib. 224, 33–47 (1999). https://doi.org/10.1006/jsvi.1998.2028

[2] Huan, R.H., Zhu, W.Q., Ma, F., Liu, Z.H.: The effect of high-frequency parametric excitation on a stochastically driven pantograph-catenary system. Shock Vib. 2014, (2014). https://doi.org/10.1155/2014/792673

[3] Han, Q., Chu, F.: Parametric instability of a Jeffcott rotor with rotationally asymmetric inertia and transverse crack. Nonlinear Dyn. 73, 827–842 (2013). https://doi.org/10.1007/s11071-013-0835-6

[4] Zaghari, B., Ghandchi Tehrani, M., Rustighi, E.: Mechanical modeling of a vibration energy harvester with time-varying stiffness. In: Proceedings of the International Conference on Structural Dynamic , EURODYN. pp. 2079–2085 (2014)

[5] Zhang, D.B., Tang, Y.Q., Liang, R.Q., Yang, L., Chen, L.Q.: Dynamic stability of an axially transporting beam with two-frequency parametric excitation and internal resonance. Eur. J. Mech. A/Solids. 85, 104084 (2021). https://doi.org/10.1016/j.euromechsol.2020.104084

[6] El-Ganaini, W.A., Kandil, A., Eissa, M., Kamel, M.: Effects of delayed time active controller on the vibration of a nonlinear magnetic levitation system to multi excitations. JVC/Journal Vib. Control. 22, 1257–1275 (2016). https://doi.org/10.1177/1077546314536753

[7] Ferrari, G., Amabili, M.: Active vibration control of a sandwich plate by non-collocated positive position feedback. J. Sound Vib. 342, 44–56 (2015). https://doi.org/10.1016/j.jsv.2014.12.019

[8] Zhang, W.: Chaotic motion and its control for nonlinear nonplanar oscillations of a parametrically excited cantilever beam. Chaos, Solitons and Fractals. 26, 731–745 (2005). https://doi.org/10.1016/j.chaos.2005.01.042

[9] Mengue, A.D., Essimbi, B.Z.: Symmetry chaotic attractors and bursting dynamics of semiconductor lasers subjected to optical injection. Chaos. 22, 13113 (2012). https://doi.org/10.1063/1.3675623

[10] Rana, S.M.S., Kulsum, U.: Bifurcation analysis and chaos control in a discrete-time predator-prey system of leslie type with simplified holling type IV functional response. Discret. Dyn. Nat. Soc. 2017, 9705985 (2017). https://doi.org/10.1155/2017/9705985

[11] Kandil, A., El-Ganaini, W.A.: Investigation of the time delay effect on the control of rotating blade vibrations. Eur. J. Mech. A/Solids. 72, 16–40 (2018). https://doi.org/10.1016/j.euromechsol.2018.03.007

[12] Kandil, A.: Study of Hopf curves in the time delayed active control of a 2DOF nonlinear dynamical system. SN Appl. Sci. 2, 1924 (2020). https://doi.org/10.1007/s42452-020-03614-0

[13] Hamed, Y.S., Kandil, A., Machado, J.T.: Utilizing macro fiber composite to control rotating blade vibrations. Symmetry (Basel). 12, 1–23 (2020). https://doi.org/10.3390/sym12121984

[14] Yang, Z., Jiang, T.: Bifurcations and Chaos in the Duffing Equation with One Degenerate Saddle Point and Single External Forcing. J. Appl. Math. Phys. 05, 1908–1916 (2017). https://doi.org/10.4236/jamp.2017.59161

[15] Jun, L.: Positive position feedback control for high-amplitude vibration of a flexible beam to a principal resonance excitation Shock Vib. 17, 187–203 (2010). https://doi.org/10.3233/SAV-2010-0506

[16] Abdelhafez, H., Nassar, M.: Suppression of Vibrations of a Forced and Self-excited Nonlinear Beam by Using Positive Position Feedback Controller PPF. Br. J. Math. Comput. Sci. 17, 1–19 (2016). https://doi.org/10.9734/bjmcs/2016/26871

[17] Hamed, Y.S., El Shehry, A., Sayed, M.: Nonlinear modified positive position feedback control of cantilever beam system carrying an intermediate lumped mass. Alexandria Eng. J. 59, 3847–3862 (2020). https://doi.org/10.1016/j.aej.2020.06.039

[18] Amer, Y.A., EL-Sayed, A.T., Abd EL-Salam, M.N.: A Suitable Active Control for Suppression the Vibrations of a Cantilever Beam. Sound Vib. 56, 89–104 (2022). https://doi.org/10.32604/sv.2022.011838

[19] Pham, P.T., Nguyen, Q.C., Yoon, M., Hong, K.S.: Vibration control of a nonlinear cantilever beam operating in the 3D space. Sci. Rep. 12, (2022). https://doi.org/10.1038/s41598-022-16973-y

[20] Li, Z., He, Y., Zhang, B., Lei, J., Guo, S., Liu, D.: Experimental investigation and theoretical modelling on nonlinear dynamics of cantilevered microbeams. Eur. J. Mech. A/Solids. 78, (2019). https://doi.org/10.1016/j.euromechsol.2019.103834

[21] Kumar, A.: Effect of approximation of curvature/inertia on the nonlinear vibrations of cantilever beam. Structures. 26, 737–744 (2020). https://doi.org/10.1016/j.istruc.2020.04.039

[22] Kandil, A., Hamed, Y.S.: Tuned Positive Position Feedback Control of an Active Magnetic Bearings System with 16-Poles and Constant Stiffness. IEEE Access. 9, 73857–73872 (2021). https://doi.org/10.1109/ACCESS.2021.3080457

[23] Kandil, A., Hamed, Y.S., Alsharif, A.M., Awrejcewicz, J.: 2D and 3D Visualizations of the Mass-Damper-Spring Model Dynamics Controlled By a Servo-Controlled Linear Actuator. IEEE Access. 9, 153012–153026 (2021). https://doi.org/10.1109/ACCESS.2021.3126868

[24] Yakovleva, T. V., Awrejcewicz, J., Kruzhilin, V.S., Krysko, V.A.: On the chaotic and hyper-chaotic dynamics of nanobeams with low shear stiffness. Chaos. 31, (2021). https://doi.org/10.1063/5.0032069

[25] Zhang, X., Wang, H., Zhao, Q., Zhou, X.: Structural modeling and dynamic analysis of the two-segment deployable beam system. Int. J. Mech. Sci. 233, 107633 (2022). https://doi.org/10.1016/j.ijmecsci.2022.107633

[26] Omidi, E., Mahmoodi, S.N.: Sensitivity analysis of the Nonlinear Integral Positive Position Feedback and Integral Resonant controllers on vibration suppression of nonlinear oscillatory systems. Commun. Nonlinear Sci. Numer. Simul. 22, 149–166 (2015). https://doi.org/10.1016/j.cnsns.2014.10.011

[27] EL-Sayed, A.T., Bauomy, H.S.: Nonlinear analysis of vertical conveyor with positive position feedback (PPF) controllers. Nonlinear Dyn. 83, 919–939 (2016). https://doi.org/10.1007/s11071-015-2377-6

[28] Niu, W., Li, B., Xin, T., Wang, W.: Vibration active control of structure with parameter perturbation using fractional order positive position feedback controller. J. Sound Vib. 430, 101–114 (2018). https://doi.org/10.1016/j.jsv.2018.05.038

[29] Abualnaja, K.M., Amer, Y.A., El-Sayed, A.T., Ahmed, E.E.E., Hamed, Y.S.: Response Analysis and Controlling the Nonlinear Vibration of Van Der-Pol Duffing Oscillator Connected to the NIPPF Controller. IEEE Access. 9, 91836–91849 (2021). https://doi.org/10.1109/ACCESS.2021.3089978

[30] Amer, Y.A., EL-Sayed, A.T., Abd EL-Salam, M.N.: On controlling of vibrations of a suspended cable via positive position feedback controller. Int. J. Dyn. Control. 11, 370–384 (2023). https://doi.org/10.1007/s40435-022-00949-x

[31] Farokhi, H., Kohtanen, E., Erturk, A.: Extreme parametric resonance oscillations of a cantilever: An exact theory and experimental validation. Mech. Syst. Signal Process. 196, 110342 (2023). https://doi.org/10.1016/j.ymssp.2023.110342

[32] Eman Desoky E. D., Kandil, A. and Kamel M.: Nonlinear Saturation Control of an Oscillatory Cantilever Beam Excited Transversely at Its Free End. Menoufia Journal of Electronic Engineering Research (MJEER), VOL 34, NO. 1, (2024). DOI: 10.21608/MJEER.2024.298923.1092

[33] Nayfeh A. H., Mook D. T.: Nonlinear Oscillations. Wiley, New York (1995). https://doi.org/10.1002/9783527617586

[34] Nayfeh A. H.: Perturbation Methods. Wiley, New York (2000). https://doi.org/10.1002/9783527617609